J Nanostruct 14(3): 800-808, Summer 2024

RESEARCH PAPER

Synthesis of Nano-CuO Powder via Sol– Gel and Investigation the Effective Factors on the Final Size

Mohsen Saadat [1], , *Omid Amiri* [2,3]*, *Mohammad GoshtasbiRad* [1]

[1] *Department of Physics, University of Sistan and Baluchestan, Zahedan, Iran*
[2] *Research Center, Cihan University Sulaimaniya, Sulaymaniyah City, 46001, Kurdistan Region, Iraq*
[3] *Medical Laboratory Analysis Department, College of Health Sciences, Cihan*

ARTICLE INFO

Article History:
Received 10 April 2024
Accepted 26 June 2024
Published 01 July 2024

Keywords:
Calcination
CuO nano powders
Sol-gel

ABSTRACT

In this investigation nano-sized copper oxide (CuO) powders have been prepared by the sol-gel method. The crystalline structure and morphology of the particles have been characterized by X-ray diffraction (XRD) and scanning electron microscopy (SEM). The results show that the different preparation conditions such as concentration of reactant, calcinations time and calcinations temperature have a significant effect on the properties of CuO nano powders. Among the factors that influence final size of particles, the calcination temperature has the most influence. Optimum sample was attained at the concentration of 0.1 molar for copper nitrate and 1 molar for Sodium hydroxide, at 160°C calcination temperature, and 3 hours calcination time. While the density of copper nitride and sodium hydroxide are 0.1 M and 1M, respectively, pure copper oxide (CuO) is obtained. By raising the portion of the copper nitride density to that of sodium hydroxide, a new phase was appeared (Cu_2O). However, the particles' size became smaller. Stirring time is lengthened and no noticeable changes in the degree of purity and the particles size occurred.

How to cite this article
Saadat M., Amiri O., GoshtasbiRad M. Synthesis of Nano-CuO Powder via Sol– Gel and Investigation the Effective Factors on the Final Size. J Nanostruct, 2024; 14(3):800-808. DOI: 10.22052/JNS.2024.03.010

INTRODUCTION

Recently nanomaterials due to their unique and symmetric characteristics in comparison with bulk materials are studied on a very large scale. Copper (II) oxide in contrast with other *oxide semiconductors* doped with *3d*-elements has a monoclinic crystal structure. CuO is a P-type semiconductor and it has a very small (1.5 ev) band gap [1, 2] and is mostly used for junction materials such as junction p-n diodes [3, 4]. The catalysts that are enriched by CuO are shown to have a very good activation for the purpose of reduction of contamination caused by NO_x [5, 6]. As a result of different characteristics of CuO and more importantly because of its nanostructure, it has numerous applications. Nano copper oxide is already used in high temperature superconductors [7, 8], optical switches [9, 10], electrode anode batteries [11, 12], heterogeneous catalysis [13-15], and gas sensors [16-18]. Recently, nanostructured CuO is made in different forms such as nanowire, nano film, nanotube and nano sphere [19]. Nano structured CuO has been synthesized by wet chemical techniques, thermal and plasma-based methods methods such as vapor chemical accumulation, electrochemical techniques and hydrothermal method [19]. These methods mostly require very expensive facilities as well as high

* *Corresponding Author Email: o.amiri1@gmil.com*

This work is licensed under the Creative Commons Attribution 4.0 International License.
To view a copy of this license, visit http://creativecommons.org/licenses/by/4.0/.

temperature environment. In this study, sol- gel method is used to produce CuO nanoparticles. The facilities needed by this method are fewer in number and they are not as expensive as those needed for other mentioned methods. More importantly, sol gel method can be carried out at room temperature and there is no need for a high temperature.

MATERIALS AND METHODS

CuO nanoparticles were synthesized through the sol-gel method. For this purpose, aquatic

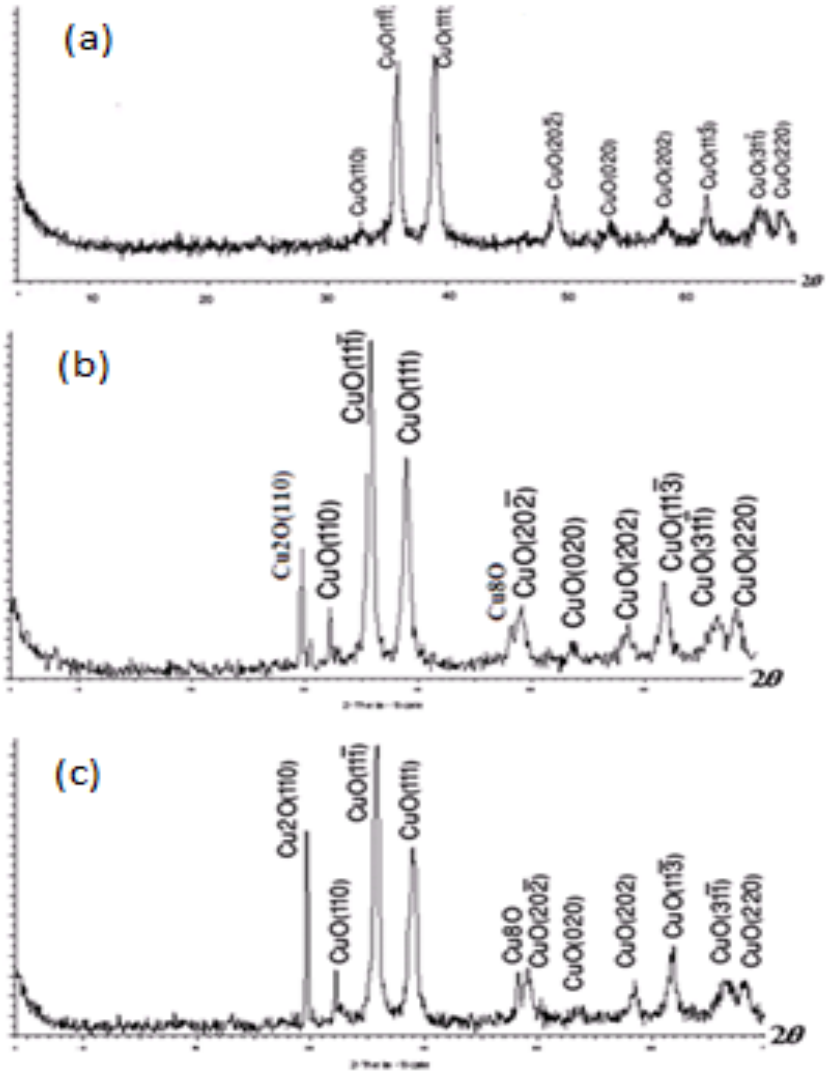

Fig. 1. XRD patterns for samples with a) copper nitride 0.1 M b) copper nitride 0.2 M c) copper nitride 0.3 M.

Table 1. The effect of different copper nitride densities on the synthesized particles mean size.

copper nitride densities	Particle mean size (nm)
0.1	37
0.2	34
0.3	31

CC BY

solutions of copper nitride and sodium hydroxide were added simultaneously at room temperature and in this way a gel is formed. The gel was washed for several times by deionized water to withdraw the nitride ions from the gel. The gel were filtered and dried at the 50 degree centigrade to obtain copper hydroxide. Then the copper hydroxide was annealed at different temperatures to achieve the final product, the copper oxide. In order to investigate the effect of the copper nitrite density, we changed the density from 0.1 molar to 0.2 and so forth. However, we keep the density of sodium hydroxide unchanged, which is 1 molar during this investigation. The samples were annealed for 3

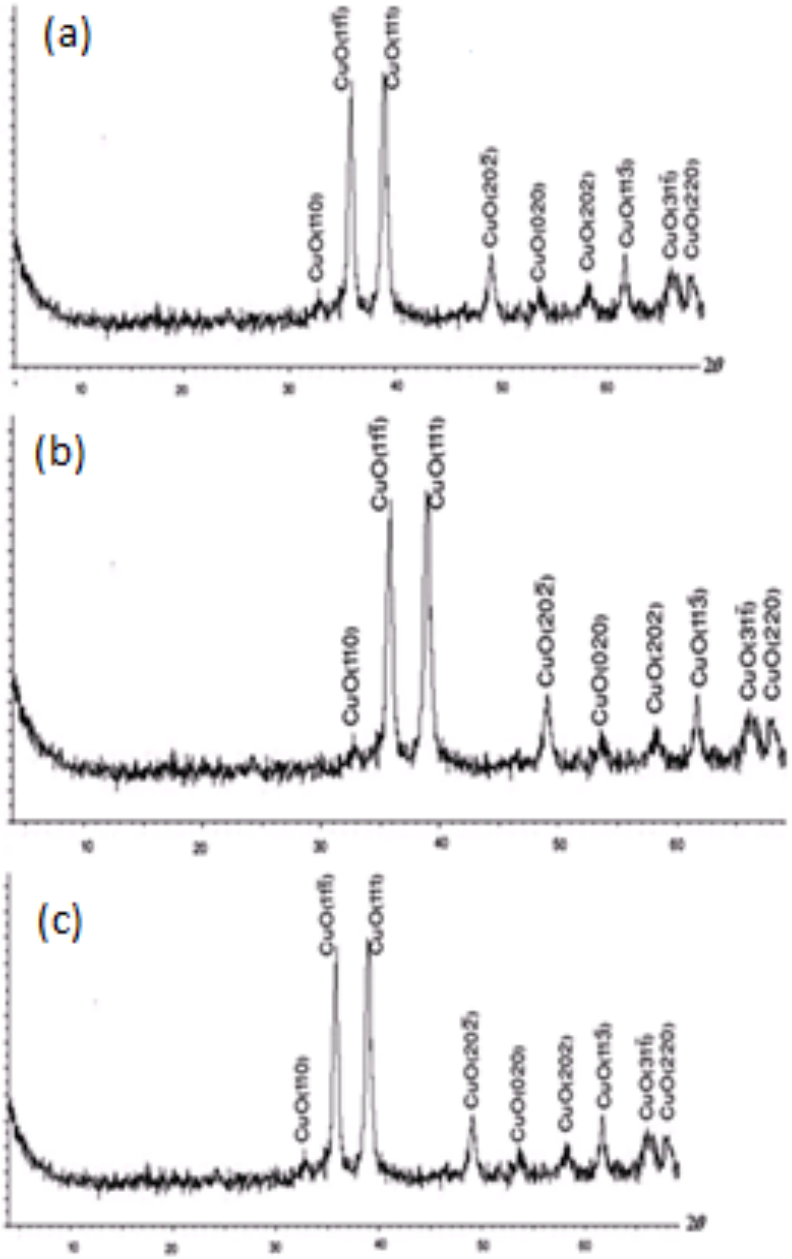

Fig 2. XRD patterns for samples with different stirring times (a) without stirring (b) 10 minutes (c) 3 hours.

CC BY

hours at 160°C. While, the density of copper nitride was 0.4 molar, the sol was not formed. Also, in this work the effect of the stirring time and the effect of time and temperature on the final product were investigated. The XRD (X- Ray Diffraction) patterns of the samples were achieved through using a diffractometer which was radiated CuK_{α}. The size of the synthesized nanoparticles was estimated by using *Scherer* equation.

RESULTS AND DISCUSSION

Effect of Copper Nitride Density

In this part of experiment, the density of copper nitride was changed from 0.1 molar to 0.2 and 0.3 molar. In Fig. 1, the XRD patterns of different samples with different copper nitride densities are shown. The figure shows that by increasing the portion of copper nitride to sodium hydroxide, the size of the particles reduced, however, the Cu_2O phase is appeared as well. The intensification of picks at 29.5° and 35.5° degrees in figure shows that by the increase in the portion of copper nitride solution over sodium hydroxide solution, leading the crystals to grow in the (111) and (110) plains of copper dioxide. The mean size of different samples is presented in Table 1.

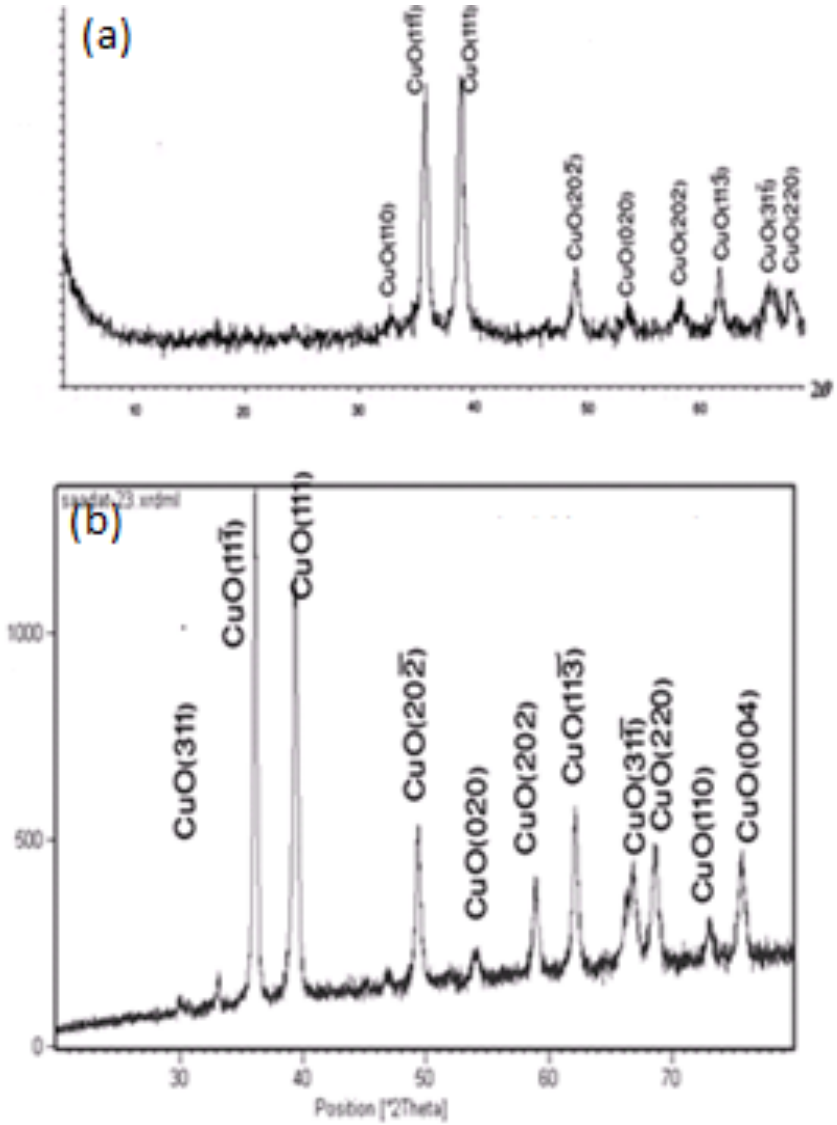

Fig 3. XRD patterns for samples with annealing times (a) 3 hours (b) 12 hours.

CC BY

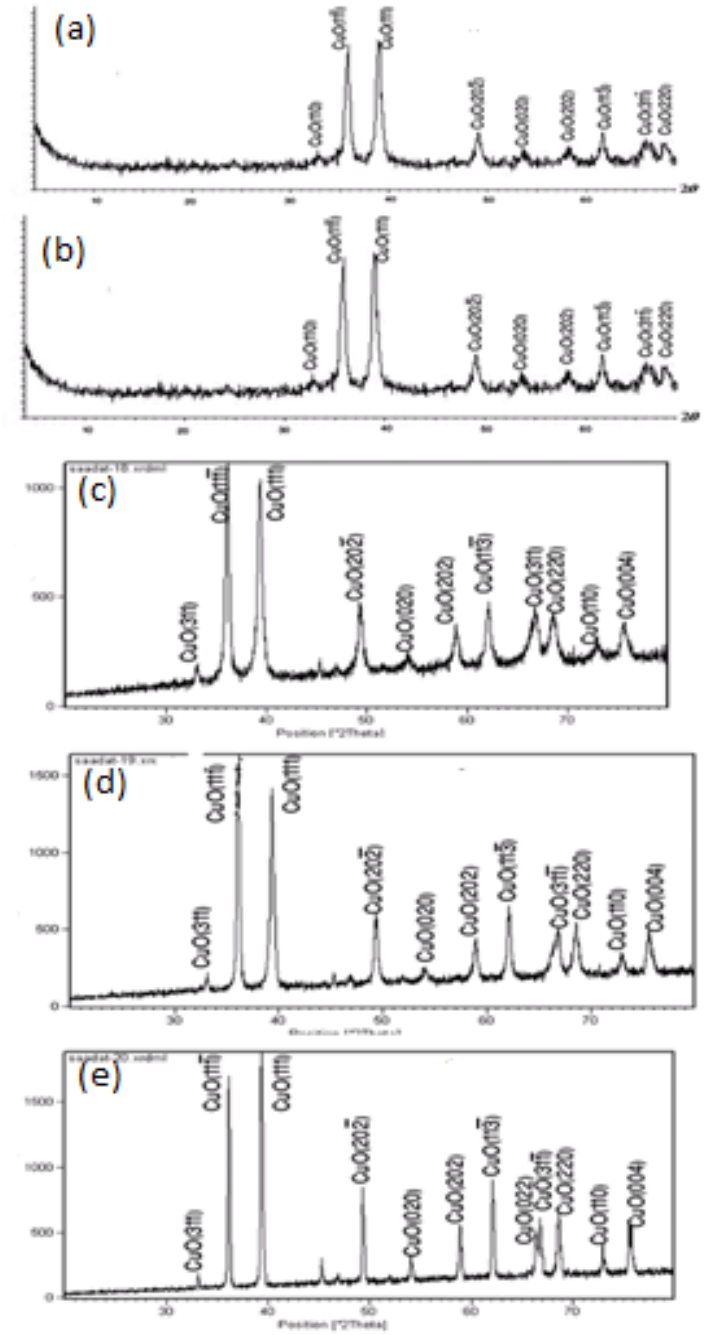

Fig. 4. XRD patterns for different Calcination Temperatures (a) 160° C (b) 180° C (c) 300° C (d) 600°C (e) 900° C.

Table 2. Effect of calcination time on the particles mean size.

Calcination time (hour)	Particle mean size (nanometer)
3	37
24	41

CC BY

Effect of Stirring time on the Sol

In this part, three samples prepared with different stirring times. One of the samples was not stirred, but other samples were stirred for 10 minutes and 3 hours, respectively. In all cases, the calcination temperature was 160° centigrade and the density of copper oxide was 0.1 molar. It is shown (in Fig. 2) that the stirring time of the

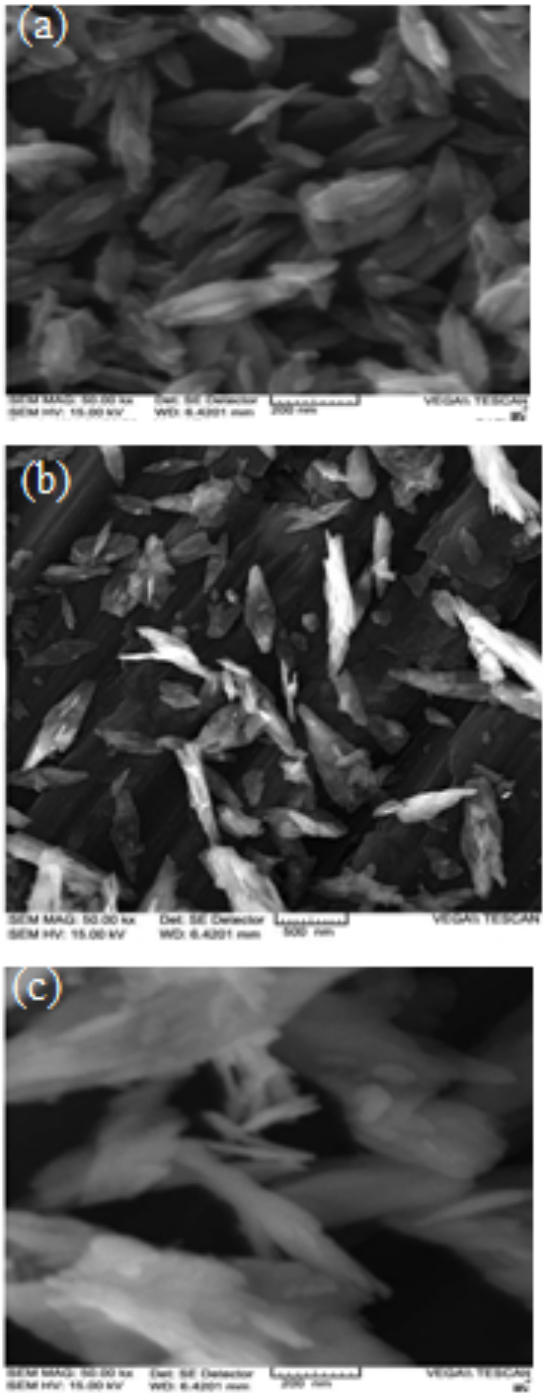

Fig. 5. SEM images for synthesized samples in different temperatures (a) 160^{o} C (b) 600^{o} C (c) 900^{o} C.

CC BY

sol did not affect the purity of the final product which proves the immediate reactions among precursors. Moreover, it can be seen that the mean size of particles in all samples are 37 nm. So, stirring time does not have any effects on the particles size too.

Effect of Calcination Time

To investigating the effect of calcination time, we changed the time from 3hours to 12 hours. As Fig. 3 shows, when the samples were annealed for a longer time, the intensity of (111) plane increased, too. Other experiment conditions like temperature and density were the same as the former one. The intensification of the (111) plain indicated that the more the calcination time, the more the growth in Cu_2O phase. Also, a rise in calcination time would lead to larger particles which prove the more growth in crystals. The mean particles size is shown in Table 2.

Calcination Temperature Effect

In this part of experiment the density of copper oxide was 0.1 M and all samples were annealed for three hours. However, the experiment is performed with four different calcination temperatures. The XRD patterns for the samples which were synthesized at temperatures of 160, 300, 600 and 900° C are depicted in Fig. 4. It can be inferred from the patterns that when the calcination

Table 3. Effect of calcination temperature on the particles mean size.

Calcination temperature (degree centigrade)	Particle mean size (nm)
160	37
180	37
300	52
600	58
900	91

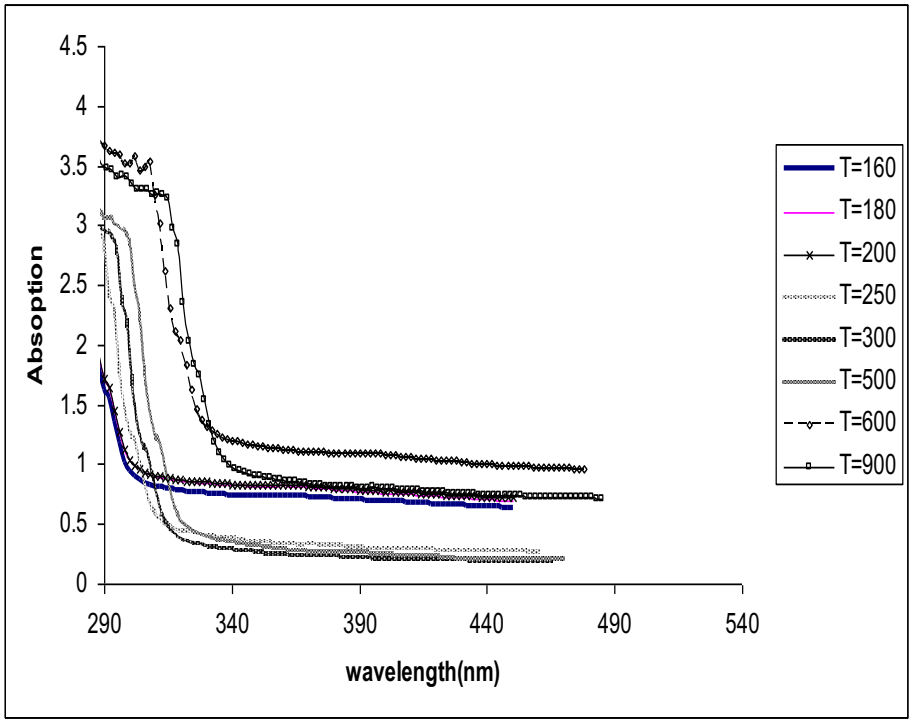

Fig. 6. UV patterns for synthesized samples in different temperatures.

CC BY

temperature was higher, the pick of the (111) plain is intensified in comparison to (111) plain. Since the pick for (111) plain of Cu_2O overlaps with the (111) CuO plane, it demonstrates the growth of the Cu_2O phase. By rising temperature to 900°C, one more pick was appeared which is due to the existence of the CuO (202) plain.

Moreover, at 900°C the intensity of the (111) plain in comparison to the (111) plain was increased which shows that in higher temperatures the crystal are grown in these crystallographic directions and the XRD pattern of nanoparticles is changed to the same pattern of the bulk copper oxide. By risingup the calcination temperature, the synthesized particles became larger and the crystals were grown larger, too. In Table 3, the size of particles is shown and in Fig. 5, the SEM images are for synthesized particles in different temperatures.

Investigation of band gap variation by temperature

For this purpose, from the samples which were synthesized at different temperatures, UV- Visible absorption spectrum was taken and the results are shown in Fig. 6.

It can be inferred from the Fig. 6 that at higher temperatures which means particle mean size is higher too, the absorption edge shifted toward the longer wavelengths. This represents that the larger the particles are, the smaller the band gap is.

CONCLUSION

While the density of copper nitride and sodium hydroxide are 0.1 M and 1M, respectively, pure copper oxide (CuO) is obtained. By raising the portion of the copper nitride density to that of sodium hydroxide, a new phase was appeared (Cu_2O). However, the particles' size became smaller. Stirring time is lengthened and no noticeable changes in the degree of purity and the particles size occurred. By increasing the calcination time at 160°, the Cu_2O phase in synthesized samples was appeared. Also, the particles were grown larger in size. The XRD pattern of the sample at 900° C is very similar to that of the bulk sample. The leaf shape and nano scale size of particles are shown by the SEM figures. The UV- Visible spectra shows that when the calcination temperature and particles mean size increases, the adsorption edge would move toward the longer wavelengths. While there has been the copper nitride 0.1 M and sodium hydroxide 1 M at 160°C, the best sample was collected.

CONFLICT OF INTEREST

The authors declare that there is no conflict of interests regarding the publication of this manuscript.

REFERENCES

1. Siddiqui H, Qureshi MS, Haque FZ. Valuation of copper oxide (CuO) nanoflakes for its suitability as an absorbing material in solar cells fabrication. Optik. 2016;127(8):3713-3717.
2. Wanninayake AP, Gunashekar S, Li S, Church BC, Abu-Zahra N. Performance enhancement of polymer solar cells using copper oxide nanoparticles. Semicond Sci Technol. 2015;30(6):064004.
3. Zhao S, Shen Y, Hao F, Kang C, Cui B, Wei D, Meng F. P-n junctions based on CuO-decorated ZnO nanowires for ethanol sensing application. Appl Surf Sci. 2021;538:148140.
4. Preda N, Costas A, Beregoi M, Apostol N, Kuncser A, Curutiu C, et al. Functionalization of eggshell membranes with CuO-ZnO based p-n junctions for visible light induced antibacterial activity against Escherichia coli. Sci Rep. 2020;10(1):20960-20960.
5. Deng Y, Shi X, Wei L, Liu H, Li J, Ou X, et al. Effect of intergrowth and coexistence CuO-CeO_2 catalyst by grinding method application in the catalytic reduction of NOx by CO. J Alloys Compd. 2021;869:159231.
6. Li H, Huang J, Yang J, Yang Z, Qu W, Xu Z, Shih K. Reduction of oxidized mercury over NOx selective catalytic reduction catalysts: A review. Chem Eng J. 2021;421:127745.
7. Tamm A, Tarre A, Verchenko V, Seemen H, Stern R. Atomic Layer Deposition of Superconducting CuO Thin Films on Three-Dimensional Substrates. Crystals. 2020;10(8):650.
8. Singh BP, Chaudhary M, Kumar A, Singh AK, Gautam YK, Rani S, Walia R. Effect of Co and Mn doping on the morphological, optical and magnetic properties of CuO nanostructures. Solid State Sciences. 2020;106:106296.
9. Wu L-f, Wang Y-h, Li P-l, Wu X, Shang M, Xiong Z-z, et al. Enhanced nonlinear optical behavior of graphene-CuO nanocomposites investigated by Z-scan technique. J Alloys Compd. 2019;777:759-766.
10. Bunea R, Saikumar AK, Sundaram K. A Comparison of Optical Properties of CuO and Cu₂O Thin Films for Solar Cell Applications. Materials Sciences and Applications. 2021;12(07):315-329.
11. Wang P, Gou X-X, Xin S, Cao F-F. Facile synthesis of CuO nanochains as high-rate anode materials for lithium-ion batteries. New J Chem. 2019;43(17):6535-6539.
12. Xu Y, Chu K, Li Z, Xu S, Yao G, Niu P, Zheng F. Porous CuO@C composite as high-performance anode materials for lithium-ion batteries. Dalton Transactions. 2020;49(33):11597-11604.
13. Sun M, Lei Y, Cheng H, Ma J, Qin Y, Kong Y, Komarneni S. Mg doped CuO–Fe_2O_3 composites activated by persulfate as highly active heterogeneous catalysts for the degradation of organic pollutants. J Alloys Compd. 2020;825:154036.
14. Walters CM, Adair KR, Hamad WY, MacLachlan MJ. Synthesis of Chiral Nematic Mesoporous Metal and Metal Oxide Nanocomposites and their Use as Heterogeneous

CC BY

Catalysts. Eur J Inorg Chem. 2020;2020(41):3937-3943.
15. Abdpour S, Santos RM. Recent advances in heterogeneous catalysis for supercritical water oxidation/gasification processes: Insight into catalyst development. Process Saf Environ Prot. 2021;149:169-184.
16. Lee JE, Lim CK, Park HJ, Song H, Choi S-Y, Lee D-S. ZnO–CuO Core-Hollow Cube Nanostructures for Highly Sensitive Acetone Gas Sensors at the ppb Level. ACS Applied Materials & Interfaces. 2020;12(31):35688-35697.
17. Chaloeipote G, Prathumwan R, Subannajui K, Wisitsoraat A, Wongchoosuk C. 3D printed CuO semiconducting gas sensor for ammonia detection at room temperature. Mater Sci Semicond Process. 2021;123:105546.
18. Patil P, Nakate UT, Nakate YT, Ambare RC. Acetaldehyde sensing properties using ultrafine CuO nanoparticles. Mater Sci Semicond Process. 2019;101:76-81.
19. Baranov O, Bazaka K, Belmonte T, Riccardi C, Roman HE, Mohandas M, et al. Recent innovations in the technology and applications of low-dimensional CuO nanostructures for sensing, energy and catalysis. Nanoscale Horizons. 2023;8(5):568-602.

CC BY